Study of Rod-Plate DC Discharge Plasma Characteristics at Atmospheric-Pressure

Thamir H. Khalaf *, **Qusay A. Abbas, Murad M. Kadhim**

Department of Physics, College of Science, University of Baghdad, Baghdad, Iraq

Abstract

The characteristics of atmospheric-pressure glow discharge (APGD) produced by rod-plate electrodes are experimentally determined. APGD is sustained by applying a high DC voltage between the electrodes. At atmospheric pressure, the shift from corona discharge to glow discharge is investigated. A rod-plate discharges configuration's volt–ampere properties show the existence of three discharge regimes: corona, glow, and spark. The variations in the electrical field distribution in the various regimes are mirrored in the discharge luminosity. The rod-plate patterns are created under a dark region, and are visible mainly due to the effect of electrons heated by the local enhanced electric field at the interface, according to the optical emission spectra of the entire discharge.

Keywords: Atmospheric-pressure plasma, V-I characteristic; Rod-Plate; Plasma parameters; Optical emission spectroscopy (OES).

دراسة خصائص بلازما تفريغ التيار المستمر للوح القضيب عند الضغط الجوي

ثامر حميد خلف* , قصي عدنان عباس, مراد محمد كاظم

قسم الفيزياء , كلية العلوم, جامعة بغداد، بغداد، العراق

الخلاصة

حددنا بشكل تجريبي خصائص تفريغ التوهج عند الضغط الجوي (APGD) التي تنتجها أقطاب لوح القضيب. يتم الحفاظ على تفريغ التوهج من خلال تطبيق جهد عالي للتيار المستمر بين الأقطاب الكهربائية. عند الضغط الجوي، يتم فحص التحول من تفريغ الهالة إلى التفريغ المتوهج. تُظهر خصائص الفولت–أمبير لتكوين تفريغات لوح القضيب وجود ثلاثة أنظمة تفريغ: الإكليل والتوهج والشرارة. تنعكس الاختلافات في توزيع المجال الكهربائي في الأنظمة المختلفة في لمعان التفريغ. يتم إنشاء أنماط صفيحة القضيب تحت منطقة مظلمة، وتكون مرئية بشكل أساسي بسبب تأثير الإلكترونات المسخنة بواسطة المجال الكهربائي المعزز الموضعي في الواجهة، وفقًا لأطياف الانبعاث البصري للتفريغ بأكمله.

_____

*Email: murad.kadhim1204@sc.uobaghdad.edu.iq

1. Introduction

The prospect of combining the benefits of plasma-based processes with the ability to generate non-thermal plasmas at atmospheric pressure without the use of vacuum equipment has sparked renewed interest [1]. The research presented in this paper focuses on a direct-current discharge in flowing atmospheric air between a rod-shaped cathode and a flat or profiled anode plate. Corona discharge will occur due to local field enhancement at the cathode of this shape. Townsend's semi-empirical expression can be used to characterize a corona discharge's volt–ampere defining feature [2].

$$I = kU (U - U_0) \tag{1}$$

where I is the total corona current, U is the voltage difference between electrodes, U_0 is the corona voltage discharge initiation, and k is an element inversely related to the gas density and dependent on the inter-electrode path length. The onset voltage U_0 is determined by the cathode rod's roundness. The lowered corona current I/U generally increases with the applied voltage. This direct link, however, only holds for low voltage values, as evidenced by the presence of a discharge in moving atmospheric air. The strain point in the lowered voltage-current characteristic marks the transition from a corona discharge to a glow discharge [3-5]. Finally, the glow discharge can spark if the voltage is raised above a critical level.

The Boltzmann plot approach is the best and broadly used spectroscopic analytical method for determining electron temperature (T_e) [6]. Boltzmann distribution is satisfied in the case of local thermodynamic equilibrium (LTE) [7].

$$Ln\left(\lambda_{ji}I_{ji}/hc\, g_jA_{ji}\right) = -E_j/kT_e + Ln(N/U) \tag{2}$$

Where: I_{ji} , λ_{ji} and A_{ji} are the intensity, wavelength and transition probability correspond to transition from j to i, g_j is a statistical weight, c is the speed of light, h is Planck constant, U is partition function, N is the density of emitting species.

The electron density (n_e) was determined using the Stark broadening impact, which necessitates a line unrestricted of self-absorption [8]:

$$n_e(cm^{-3}) = [\Delta\lambda/2\omega_s]\, N_r \tag{3}$$

ω_s is the electron impact value, that can be found in the standard tables, N_r is the reference electron density, and $\Delta\lambda$ is the line's full width at half maximum (FWHM). The electrons in the Debye sphere are thought to be the source of the shielding, whose number is given by [9]:

$$N_D = 1.38 \times 10^6 \frac{[T_e\ (°K)]^{3/2}}{[n_e\ (cm^{-3})]^{1/2}} \tag{4}$$

2. Experimental part

Figure1 shows a schematic diagram of the rod–plate electrodes DC glow discharge system at atmospheric air pressure. The cathode is a brass rod positioned above a grounded anode with varying cathode-anode gap distance of (1, 2, 3, and 4mm). The rod is of 10cm length with different diameters (4, 5, and 6mm). The grounded anode is a circular plate of 9.5cm diameter. In this study, a DC constant voltage of almost 20kV was implemented between the two electrodes to generate the discharge. The external voltage

causes the plasma discharge, and the voltage of the electrodes falls as a result. The Optical Emission Spectrometer (OES) (purchased from Thorlabs) was used to measure the emission spectrum released by the plasma in order to diagnose spatially integrated plasma light emissions in the 320-740nm wavelength range in order to evaluate plasma properties. The properties of the plasma generated in the inter-electrodes gap were estimated using the findings of this system's spectral region, which were adjusted employing NIST database management system.
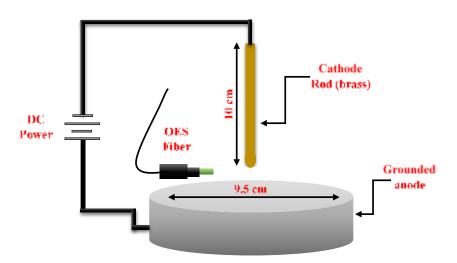

Figure 1: A schematic diagram of the rod-plate cathode DC discharge setup.

3. Results and discussions

Figure 2(a) demonstrates the changes of voltage and current with the change of the cathode-anode distance for the different values of the cathode diameter. as the variation of voltage and current with the distance between the electrodes of a DC discharge plasma for different values of the cathode diameter. The discharge current is increased by gradually increasing the voltage while the electrode spacing is increased from 1 to 4mm. Increasing the current voltage amount to a critical level. Then, as the diameter of the cathode rod increases from 4 to 6mm, a rapid current drop (or jump) occurs, followed by a maximum voltage increase. As the distance between the electrodes grows, a slightly higher voltage is required to maintain a glow discharge, resulting in an increase in the discharge voltage across the gap, which multiplies the discharge across the gap. Images of rod–plate electrodes have also been taken for numerous discharges spacing in parallel to the voltage–current attribute, as seen in Figure 2(b).
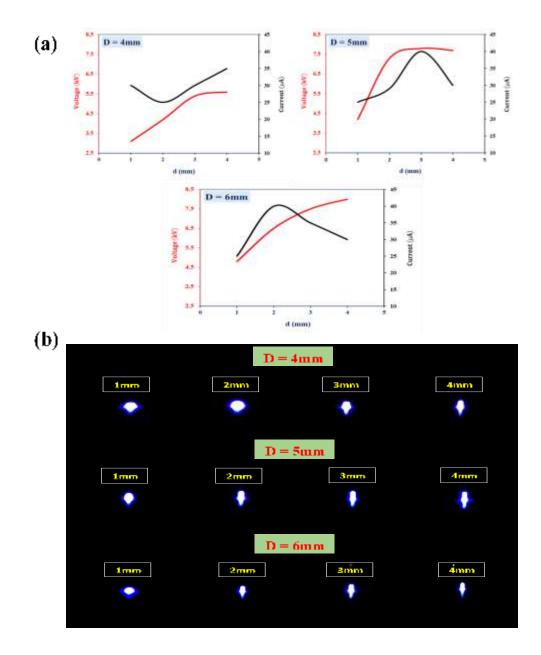
Figure 2: (a) The variation of voltage and current with the distance between the electrodes, and (b) the pictures of the corresponding rod-plate electrodes obtained for different discharge distances.

The optical emission spectra of plasma produced in the gap between the electrodes at atmospheric air pressure, for different gap distances (1, 2, 3, and 4mm) with three different cathode diameters (4, 5, and 6mm) are shown in Figure 3. One can observe from these spectra many peaks of the nitrogen atomic (N I) lines and the ionic emission lines of the nitrogen (N II) at different wavelengths. These peaks are of different intensities because of the varying probability of transition and the exciting levels of statistical weight. The intensity of the peaks increased with the decrease of the distance between the electrodes, with a higher rate when the cathode diameter was reduced from 6 to 4mm, because it leads to more ionization collisions due to an increase in the potential difference between the electrodes, which allows electrons to have enough excitation energy.
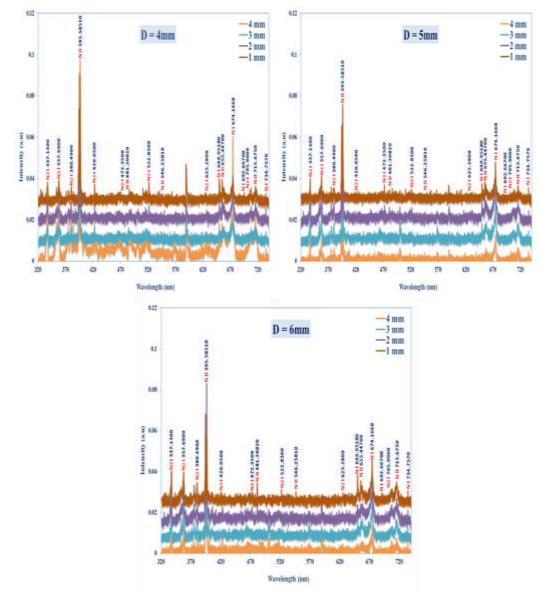
Figure 3: The optical emission spectra of rod-plate DC discharge plasma system, at atmospheric air pressure.

The value of T_e was estimated using the Boltzmann plot technique (Equation (2)) where the wavelength of the (N I) emission lines (listed in Table 1) were used. The values of T_e is equal to the reciprocal of the slope of the best fitted line of the plot of $Ln(\lambda_{ji} I_{ji}/hc\, g_j A_{ji})$ versus highest energy level (E_j) [10]. Peaks from the same atomic species must be compared to NIST data.

Table 1: N I standard lines are used to calculate T_e, and their characteristics [11].

λ(nm)	$A_{mn} \times g_m$	E_i(eV)	E_j(eV)
649.9518	70.8×10^5	11.7575319	13.6645956
692.6670	46.5×10^5	11.8397086	13.6291690
674.1668	6.2×10^5	11.8397086	13.6782741
734.7570	33.3×10^6	12.0096116	13.6965647

Figure 4 shows the Boltzmann plots using the selected atomic nitrogen lines (N I) for the rod-plate discharge system, in the cases under study at different gap distances (1, 2, 3, and 4mm) and different cathode diameters (4, 5, and 6mm).
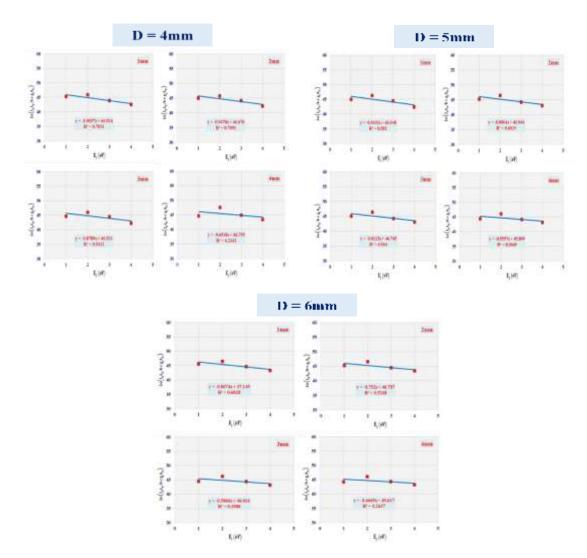

Figure 4: Boltzmann plots for N I peaks at varying gap distances (1, 2, 3, and 4mm) with different cathode diameters (4, 5, and 6mm).

Equation (3), also known as the Stark broadening impact, could be used to determine n_e. Based on typical values of the broadening for this line, FWHM values were used to compute n_e using the Stark effect ($N_r = 10^{16} cm^{-3}$) [12-14].

Figure 5 shows that the electron temperature (T_e) increases with increase in the inter-electrodes gap (from 1 to 4mm). In contrast, when the spacing between the electrodes rises, electron number density (n_e) decreases, resulting in a lower likelihood of ionization collisions. In addition, the T_e increases exponentially with the increase in cathode diameter (from 4 to 6mm), While the n_e decreases dramatically, as shown in Table 2.
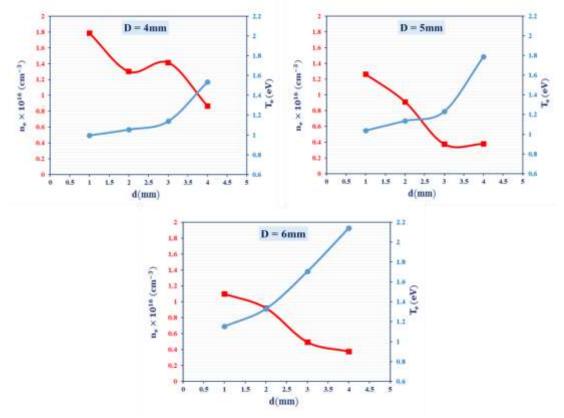

Figure 5: The Variation of n_e and T_e of the plasma emitted from rod-plate electrodes as a function of the distance between the electrodes for different cathode diameters.

Table 2: Plasma parameters of atmospheric-pressure DC glow discharge in rod–plate electrodes.

D (mm)	d (mm)	T_e (eV)	$n_e \times 10^{16}$ (cm^{-3})	N_D
4	1	0.9963	1.7859	12830
	2	1.0551	1.3008	16383
	3	1.1378	1.4139	17598
	4	1.5342	0.8647	35234
5	1	1.0383	1.2631	16230
	2	1.1358	0.9137	21833
	3	1.2311	0.3759	38412
	4	1.7867	0.3780	66973
6	1	1.1529	1.0996	20353
	2	1.3298	0.9216	27541
	3	1.7047	0.4932	54642
	4	2.1418	0.3749	88263

Conclusions

In this work, the features of the rod-plate plasma were examined as a response to the applied DC voltage, the air gap between the electrodes, and the cathode rod diameter. Related to the current-voltage characteristics of a rod-plate discharge and the emission intensities from nitrogen atoms of the atomic (N I) lines and the ionic emission lines (N II), as the increase in the applied voltage leads to an increase in the discharge current. The best optical emission intensities from N I at a given voltage were probed using an OES, denoting that increased electron density is caused by excess power consumption in the plasma, and further increase in the air gap reduced the power usage.

References

[1] E. E. Kunhardt, "Generation of large-volume, atmospheric-pressure, nonequilibrium plasmas,"*IEEE transactions on plasma science*, vol. 28, no. 1, PP. 189-200, 2000.
[2] J. S. Townsend, "The potentials required to maintain currents between coaxial cylinders," The London, Edinburgh, and Dublin Philosophical Magazine and Journal of Science, vol. 28, no. 163, PP. 83-90, 1914.
[3] Y. S. Akishev, M. E. Grushin, I. V Kochetov, A. P. Napartovich, M. V. Pan'kin, and N. I. Trushkin, "Transition of a multipin negative corona in atmospheric air to a glow discharge," *Plasma Physics Reports*, vol. 26, no. 2, pp. 157-163, 2000.
[4] Y. Akishev, O. Goossens, T. Callebaut, C. Leys, A. Napartovich, and N. Trushkin, "Pin-to-plate glow discharge in flowing air at atmospheric pressure," In Proceedings HAKONE VII, International Symposium on high pressure low temperature plasma chemistry, Greifswald, pp. 13-17, 2000.
[5] Y. Akishev, O. Goossens, T. Callebaut, C. Leys, A. Napartovich, and N. Trushkin, "The influence of electrode geometry and gas flow on corona-to-glow and glow-to-spark threshold currents in air," *Journal of Physics D: Applied Physics*, vol. 34, no. 18, pp. 2875, 2001.
[6] N. Idris, T. N. Usmawanda, K. Lahna, and M. Ramli, "Temperature estimation using Boltzmann plot method of many calcium emission lines in laser plasma produced on river clamshell sample," *Journal of Physics: Conference Series*, vol. 1120, no. 1, pp. 1-11, 2018.
[7] T. Hussain, M. A. Gondal, and M. Shamraiz, "Determination of plasma temperature and electron density of iron in iron slag samples using laser induced breakdown spectroscopy," In IOP Conference Series: Materials Science and Engineering, vol. 146, no. 1, pp. 1-11, 2016.
[8] S. A. Abbasi, M. Rafique, A. A. Mir, K. J. Kearfott, S. Ud-Din Khan, T.M. Khan and J. Iqbal, "Quantification of elemental composition of Granite Gneiss collected from Neelum Valley using calibration free laser-induced breakdown and energy-dispersive X-ray

spectroscopy," *Journal of Radiation Research and Applied Sciences*, vol. 13, no. 1, pp. 362-372, 2020.

[9] F. F. Chen, "Introduction to plasma physics and controlled fusion," 3rd ed., New York, Springer, 1984.

[10] H. Park, S. J. You, , and W. Choe, "Correlation between excitation temperature and electron temperature with two groups of electron energy distributions," *Phys. Plasmas,* vol. 17, no. 10, pp. 1–4, 2010.

[11] NIST Atomic Spectra Database." [Online]. Available: https:// www.nist.gov/pml/atomic-spectra-database, 2020.

[12] N. Konjevic, A. Lesage, J. Fuhr, and W. Wiese, "Experimental Stark widths and shifts for spectral lines of neutral and ionized atoms(A Critical Review of Selected Data for the Period 1989 Through 2000)," *J. Phys. Chem. Ref. Data*, vol. 31, no. 3, pp. 819-927, 2002.

[13] T. A. Hameed, and S. J. Kadhem, "Plasma diagnostic of gliding arc discharge at atmospheric pressure," *Iraqi Journal of Science*, vol. 60, no. 12, pp. 2649-2655, 2019.

[14] Y. K. Jabur, M. G. Hammed, and M. K. Khalaf, "DC Glow Discharge Plasma Characteristics in Ar/O2 Gas Mixture," *Iraqi Journal of Science,* vol. 62, no. 2, PP. 475-482, 2021.